Assessment of Adeno-Associated Virus Serotype Tropism in Human Retinal Explants

Luke A. Wiley,[1,2] Erin R. Burnight,[1,2] Emily E. Kaalberg,[1,2] Chunhua Jiao,[1,2] Megan J. Riker,[1,2] Jennifer A. Halder,[1,2] Meagan A. Luse,[1,2] Ian C. Han,[1,2] Stephen R. Russell,[1,2] Elliott H. Sohn,[1,2] Edwin M. Stone,[1,2] Budd A. Tucker,[1,2] and Robert F. Mullins[1,2,*]

[1]Stephen A. Wynn Institute for Vision Research and [2]Department of Ophthalmology and Visual Sciences, Carver College of Medicine, University of Iowa, Iowa City, Iowa.

Advances in the discovery of the causes of monogenic retinal disorders, combined with technologies for the delivery of DNA to the retina, offer enormous opportunities for the treatment of previously untreatable blinding diseases. However, for gene augmentation to be most effective, vectors that have the correct cell-type specificity are needed. While animal models are very useful, they often exhibit differences in retinal cell surface receptors compared to the human retina. This study evaluated the use of an *ex vivo* organotypic explant system to test the transduction efficiency and tropism of seven different adeno-associated virus type 2 (AAV2) serotypes in the human retina and retinal pigment epithelium-choroid—AAV2/1, AAV2/2, AAV2/4, AAV2/5, AAV2/6, AAV2/8, and AAV2/9—all driving expression of GFP under control of the cytomegalovirus promoter. After 7 days in culture, it was found that AAV2/4 and AAV2/5 were particularly efficient at transducing photoreceptor cells and that AAV2/5 was highly specific to the outer nuclear layer, whereas AAV2/8 displayed consistently low transduction of photoreceptors. To validate the authenticity of the organotypic culture system, the transduction of the same set of AAVs was also compared in a pig model, in which sub-retinal injections *in vivo* were compared to cultured and transduced organotypic cultures *ex vivo*. This study shows how different AAV serotypes behave in the human retina and provides insight for further investigation of each of these serotypes for gene augmentation–based treatment of inherited retinal degeneration.

Keywords: adeno-associated virus, serotype, human retina, explant, photoreceptors

INTRODUCTION

HERITABLE DISEASES OF THE RETINA that lead to photoreceptor cell degeneration are an important cause of vision loss, and many of these monogenic disorders have a very early onset. Retinal diseases such as retinitis pigmentosa (RP) and Leber congenital amaurosis (LCA) are also very heterogeneous; that is, each clinical entity can be caused by mutations in any of dozens of different genes. For example, the authors' group recently carried out molecular investigation of 1,000 consecutive families with inherited retinal disease seen in a single clinic and found that the 760 disease-causing genotypes observed were distributed across 104 different genes.[1] While the challenges in developing therapies for such a large number of genes are great, the retina does offer the advantage, compared to other tissues in the central nervous system (CNS), that it is a relatively accessible compartment for delivery of therapeutic agents.

More than 15 years ago, researchers took advantage of this accessibility and the non-pathogenicity of adeno-associated virus (AAV) to deliver AAVs to the sub-retinal space and demonstrated that AAV-mediated gene replacement therapy could restore vision in a canine model of *RPE65*-associated LCA.[2] The efficacy demonstrated in the canine model paved the way for human trials in patients with the same disorder that have proved safe and efficacious.[3–5] A single sub-retinal injection of AAV2 (serotype 2) was shown to be well-tolerated and sufficient to induce prolonged

*Correspondence: Dr. Robert F. Mullins, Stephen A. Wynn Institute for Vision Research and Department of Ophthalmology and Visual Sciences, Carver College of Medicine, University of Iowa, 375 Newton Road, Iowa City, IA 52242. E-mail: robert-mullins@uiowa.edu

DOI: 10.1089/hum.2017.179

expression of RPE65 protein in humans, and to result in improvement in visual acuity, pupillary light reflex, visual fields, and ambulatory vision that was closely correlated with the area of the retina that received treatment.[6] Further, no adverse immune responses or extra-ocular spread of AAV2-*RPE65* was detected.[6] These encouraging results created tremendous interest throughout the ophthalmic research community in the investigation of gene augmentation and additional AAV serotypes that could be potentially useful as therapeutic vehicles. Notably, >75% of the genes identified in the authors' recent 1,000-family study have coding sequences small enough to fit into an AAV.[1]

One important feature of *RPE65*-associated LCA is that the responsible gene is expressed solely by the retinal pigment epithelium, which is highly phagocytic and may be more susceptible to viral transduction than retinal neurons.[7–9] For most other retinal degenerative diseases, the defective gene product is likely to be expressed in the photoreceptor cells. In most patients, there will also be some degree of photoreceptor cell death and altered retinal morphology. As a result, when developing an array of gene augmentation–based therapies, one will need to be able to choose from a variety of tropic behaviors to be able to effect the greatest benefit in a variety of diseases and disease states.

In order to determine the efficiency and tropism of different AAV serotypes toward photoreceptor cells, investigators have evaluated a variety of animal model species, including but not limited to mice and rats,[10–15] pigs,[9,16,17] dogs,[18–20] and nonhuman primates.[18,21–24] One limitation of the direct application of results from animal studies is that viral transduction can vary widely across species.[25] While animal studies have been valuable in showing efficacy for the treatment of diseases like *RPE65*-associated LCA, optimization of viral vectors would benefit from studies in human cells.

The current study demonstrates the use of an organotypic explant approach to test the viral transduction efficiency and tropism of seven different AAV serotypes in human retina and RPE-choroid: AAV2/1, AAV2/2, AAV2/4, AAV2/5, AAV2/6, AAV2/8, and AAV2/9. The study shows that while there is evidence of variability in outer nuclear layer (ONL) transduction efficiency across different donor retinas, this approach provides a robust means of determining how each AAV serotype transduces human retina. This study will pave the way for further investigation of each of these serotypes for replacement of retinal disease–causing genes in humans.

MATERIALS AND METHODS

Ethics statement

Human donor eyes were collected as part of a research eye collection at the Wynn Institute for Vision Research. All samples were obtained from the Iowa Lions Eye Bank after full consent of the donors' families and in accordance with the Declaration of Helsinki. All pig experiments were conducted with the approval of the University of Iowa Animal Care and Use Committee (animal welfare assurance #7051070) and were consistent with the ARVO Statement for the Use of Animals in Ophthalmic and Vision Research.

Preparation of human retinal explants

Human donor eyes (Table 1) were obtained from the Iowa Lions Eye Bank (Coralville, IA) within 4–6 h of death. The anterior segment, lens and vitreous, were removed from each eye, leaving posterior eyecups consisting of intact neural retina, choroid, and sclera. Retinal tissue was collected using a 5 mm biopsy punch and cultured in six-well transwell culture plates with the photoreceptor cell layer down (Corning Life Sciences, Tewksbury, MA; cat. no. 3412). Retinal explants were maintained in neural retinal medium (Neurobasal Medium; Thermo Fisher Scientific, Waltham, MA; cat. no. 21103049), with 1% N-2 Supplement (Thermo Fisher Scientific; cat. no. 17502048), 2% B-27 Supplement (Thermo Fisher Scientific; cat. no. 17504044), 1% GlutaMAX Supplement (Thermo Fisher Scientific; cat. no. 35050-061), 50 μg/mL of recombinant human beta-NGF (R&D Systems, Minneapolis, MN; cat. no. 256-GF-100), and 50 μg/mL recombinant human EGF (R&D Systems; cat. no. 236-EG-200) for 7 days at 37°C and 5% CO_2, with media changes performed every other day. None of the eyes used for these studies exhibited any gross pathology.

Preparation of RPE-choroid organ cultures

In order to identify the optimal vectors for transducing human RPE and choroidal cells, RPE-choroid organ cultures were established as described previously.[26] Briefly, RPE-choroid samples were isolated from a single human donor eye (age 96 years) using a 5 mm biopsy punch, as described above, and cultured in Dulbecco's modified Eagle's medium (Thermo

Table 1. *Human donors*

Donor eye	*Age*	*Sex*	*Cause of death*
1	37	Female	Acute liver failure
2	84	Female	Aspiration pneumonia
3	96	Female	Sepsis
4	56	Male	Cardiac arrest

Fisher Scientific; cat. no. 11965-092) with 5% fetal bovine serum (Thermo Fisher Scientific; cat. no. 26140-079) and 1% penicillin streptomycin (Thermo Fisher Scientific; cat. no. 15140-122) for 7 days at 37°C and 5% CO_2. These cultures maintain vascular and RPE differentiation markers and RPE tight junctions for several days.[26]

AAV vector production

Recombinant AAV2 vectors expressing enhanced green fluorescent protein (eGFP) under control of the cytomegalovirus (CMV) promoter were packaged by the University of Iowa Gene Transfer Vector Core into capsids with the following serotypes: AAV2/1 (AAV1), AAV2/2 (AAV2), AAV2/4 (AAV4), AAV2/5 (AAV5), AAV2/6 (AAV6), AAV2/8 (AAV8), and AAV2/9 (AAV9).

Viral transduction of human retinal explants and RPE-choroid organ cultures

Three independent experiments were performed, each using a different human donor eye (Table 1, Donor Eyes 2–4). A brief summary of this procedure is depicted in Fig. 1. Each AAV serotype was evaluated in duplicate retinal explants cultured in the same transwell insert in a six-well plate. AAV serotypes were titer matched to within one-half log of one another (Table 2). For each serotype, 10 μL of AAV was injected directly beneath each of the two retinal explants, creating a bleb similar to that formed *in vivo* when performing therapeutic subretinal injections. An additional 10 μL of virus was added to the culture medium that was placed beneath the transwell insert (*i.e.*, a total of 20 μL of AAV was delivered per well). The total number of vector genomes per transwell for each serotype is listed in Table 2. The identity of each serotype was masked both to the individual applying the virus and to the individual processing and analyzing the data. The data were only unmasked following the completion of the study. As indicated above, retinal explants and RPE-choroid organ cultures were maintained for 7 days post transduction.

Sub-retinal injection of AAVs into wild-type mini-swine

All animal procedures were performed in accordance with the ARVO Statement for the Use of Animals in Ophthalmic and Visual Research. Under general anesthesia, 6-month-old wild-type mini pigs underwent pars plana vitrectomy using a 23-gauge instrument, which included induction of posterior vitreous detachment (Alcon Accurus Vitrector). A 41-gauge flexible polyamide cannula was used to create a small retinotomy to allow a 300 μL sub-retinal bleb containing each AAV serotype (3×10^{11} IU) to be injected beneath the central, cone-rich visual streak. Sclerotomies were sutured, and 5% povidone-iodine was used to rinse the eye. Each AAV serotype was injected into three independent eyes. Seven days after injection, the pigs were euthanized via overdose of sodium pentobarbital (euthasol). Injected eyes were enucleated, and posterior poles were processed for immunohistochemistry (below). An additional set of retinal punches was collected on the opposite side of the optic nerve from the injection site. These punches were used to generate retinal explants that were cultured and exposed to AAVs, as described above for human eyes. Punches taken as explants were well outside of the areas affected by the AAV injection in all cases.

Viral transduction of pig retinal explants

Pig retinal explants were collected with a 5 mm biopsy punch, cultured, and treated with each AAV serotype, as described above for human retinal explants.

Immunohistochemistry and confocal microscopy of AAV-treated explants

After 7 days of culture, retinal explants were rinsed in 1×phosphate-buffered saline (PBS) and fixed for 2 h in 4% paraformaldehyde. Explants were embedded in 4% low-melting temperature agarose (Research Products International Corp., Mount Prospect, IL; cat. no. A20070-100.0) and sectioned at a thickness of 100 μm using a vibrating tissue slicer (Leica VT1000 S Vibratome; Leica Microsystems, Wetzlar, Germany). Sections were blocked in immunocytochemical blocking buffer, as described previously,[27] and were labeled with rat anti-GFP antibody (BioLegend, San Diego, CA; cat. no. 338002) overnight at 4°C and rinsed the next day in wash buffer (1×PBS, Thermo Fisher Scientific; 0.2% Tween® 20, Sigma–Aldrich, S. Louis, MO, cat. no. P2287). Samples were subsequently incubated in goat anti-rat Alexa Fluor 488 secondary antibody (Thermo Fisher Scientific; cat. no. A-11006) for 2 h at room temperature in immunocytochemical blocking buffer followed by additional rinses in wash buffer. Labeled thick sections were mounted in polyvinyl alcohol (PVA)-based mounting medium containing 1,4-diazabicyclo[2.2.2]octane (DABCO), 100 μg/mL of PVA (Sigma–Aldrich; cat. no. 341584), 25% v/v glycerol (Sigma–Aldrich; cat. no. G9012), 0.1 M Tris-HCl, pH 8–8.5, 25 μg/mL DABCO (Sigma–Aldrich; cat. no. 290734), and 4′,6-diamidino-2-phenylindole dihydrochloride (DAPI; Sigma–Aldrich; cat. no. D9542; 1:10,000 dilution). Labeled sections were visualized using a Leica TCS SPE DMi8 in-

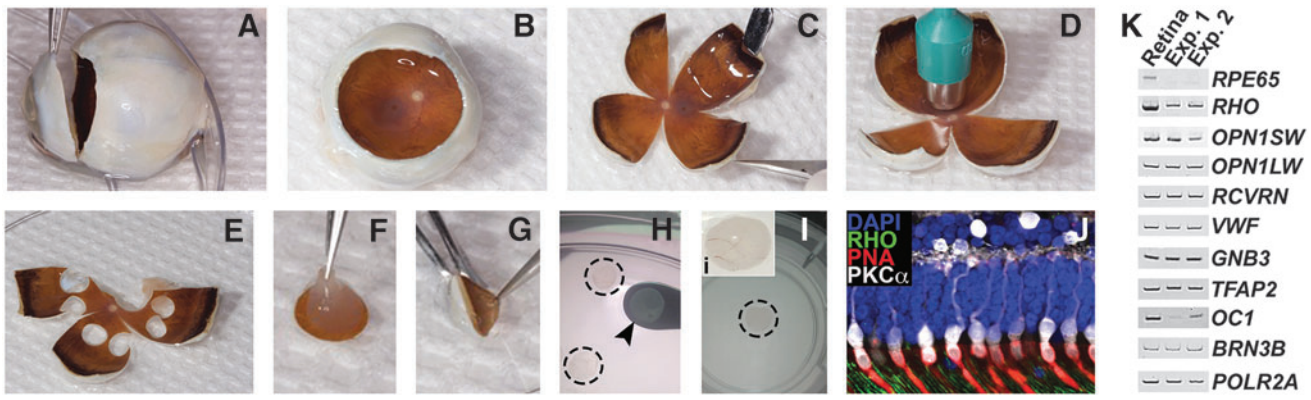

Figure 1. Human donor eye dissection and culture of retinal explants. **(A** and **B)** Fresh human donor eyes were cut along the circumference of the limbus **(A)** and the cornea and lens were removed, leaving the posterior eyecup consisting of the vitreous gel, neural retina, RPE-choroid, and sclera **(B)**. **(C–E)** Posterior eyecups were cut into "clover leaves" **(C)** and a 5 mm biopsy punch **(D)** was used to isolate punches of peripheral neural retina, RPE-choroid, and sclera **(E)**. **(F–I)** Individual punches were mechanically separated into neural retinal **(F)** and RPE-choroidal **(G)** layers. Neural retinal explants were transferred using a micro-spatula **(H**; *dashed outlines***)** to transwell inserts **(I** and **i)**, treated with adeno-associated virus (AAV) serotypes and cultured for 7 days. **(J)** Immunohistochemical analysis of explants demonstrated that retinal architecture was well-preserved following 7 days in culture. Positive labeling of rod (anti-rhodopsin antibody; RHO; *green*) and cone (rhodamine peanut agglutinin; PNA; *red*) outer segments, as well as cone bipolar connections with the inner retina were evident (anti-protein kinase subunit C, alpha antibody; PKCα; *white*). Nuclei were counterstained with DAPI (*blue*). **(K)** Reverse transcription polymerase chain reaction analysis comparing fresh human donor retina to an explanted retinal punch from the same individual (Table 1, Donor Eye 1) after 7 days in culture. Transcripts were chosen to assess the expression of retinal cell type-specific genes representing the outer and inner retina: photoreceptor cells (*RHO*, *OPN1SW*, *OPN1LW*, and *RCVRN*), retinal vascular endothelium (*VWF*), bipolar cells (*GNB3*), amacrine cells (*TFAP2*), horizontal cells (*OC1*), and ganglion cells (*BRN3B*). *RPE65* was used as a control for purity of the retinal explant (*i.e.*, RPE contamination), and *POLR2A* served as a loading control.

verted confocal microscope system (Leica Microsystems).

Quantification of ONL transduction in human retinal explants

For imaging immunolabeled explants, the investigator performing confocal microscopy was masked to the AAV serotype. The areas of the ONL were selected using the DAPI channel only. Only after choosing an area for image acquisition was the 488 channel acquired. For each independent experiment, at least three sections were evaluated, and three z-stacks were collected in non-overlapping fields within each section. For quantitative analysis, 100 μm z-stacks (using 1 μm steps) were acquired using the DAPI and 488 channels. In addition, the LAS X 3D software (Leica Microsystems) was employed to trim the first 20 μm from each z-stack to ensure consistent depth for comparison between explants within the same experiment, as well as between independent experiments. The LAS X 3D software was used to calculate the number of ONL nuclei per z-stack using the DAPI channel and to count the number of GFP-positive cells manually. The percentage of transduced cells was then calculated for each z-stack (*i.e.*, GFP-positive nuclei/total nuclei $\times$ 100%).

Table 2. *Viral titers*

Serotype	*Titer (vg/mL)*	*Total vg/well*
AAV1	1.8×10^{12}	5.4E+10
AAV2	1.3×10^{13}	3.9E+10
AVV4	2.7×10^{12}	8.1E+10
AAV5	1.7×10^{13}	5.1E+10
AAV6	2.8×10^{12}	9.45E+10
AAV8	5.4×10^{13}	1.6E+11
AAV9	4.6×10^{13}	1.4E+11

AAV, adeno-associated virus.

Assessment of AAV tropism in inner retina

Inner retinal tropism for each AAV serotype was evaluated qualitatively by recording whether cells of the inner nuclear layer (INL) or ganglion cell/nerve fiber layers (GCL/NFL) were GFP-positive in each 100 μm z-stack. The percentage of z-stacks displaying GFP expression in the INL or GCL/NFL for each independent experiment (*i.e.*, each of three donor eyes), and the overall percentage of z-stacks with GFP-positive labeling within the INL or GCL/NFL across the three independent donor eyes, was evaluated.

Immunohistochemistry of AAV-treated human RPE-choroid organ cultures

Organ cultures of RPE-choroid were fixed in 4% paraformaldehyde prior to embedding and sectioning on a cryostat. Sections were labeled with antibodies directed against CD45 (BD Biosciences, San Jose, CA; cat. no. 555480) and/or the lectin

Ulex europaeus agglutinin-I (Vector Laboratories, Burlingame, CA; cat. no. B-1065), as described previously.[28] In addition, sections were labeled with rat anti-GFP (BioLegend, San Diego, CA; cat. no. 338002). Sections were evaluated using epifluorescence microscopy.

Reverse transcription polymerase chain reaction

In order to assess preservation of retina cell type-specific transcripts, retinal explant cultures from a 37-year-old donor were established, and compared to flash frozen retina from the same eye. After 1 week of culture, total RNA was isolated from both cultured and uncultured tissue using the RNeasy Mini kit (Qiagen, Germantown, MD; cat. no. 74106) according to the manufacturer's instructions. One hundred nanograms of RNA template was amplified in one-step reverse transcription polymerase chain reactions (RT-PCR) using the Superscript III One-Step RT-PCR System (Life Technologies/Thermo Fisher Scientific; cat. no. 12574018), with primers hybridizing to human retinal transcripts listed in Supplementary Table S1 (Supplementary Data are available online at www.liebertpub.com/hum).

RESULTS

Explanted human donor retinas retain normal architecture and expression of retinal cell type-specific transcripts

In order to determine the transduction efficiency of AAVs in human retina, seven different AAV serotypes were tested using the *ex vivo* organotypic explant strategy outlined in Fig. 1. Seven days after plating, cultured retina retained normal architecture, including intact rod and cone photoreceptor inner and outer segments, a full ONL, and outer-to-inner retinal connectivity (Fig. 1J). Moreover, explants cultured for 7 days expressed the same retinal cell type-specific transcripts as the flash-frozen tissue from the same donor retina (Table 1, Donor 1) that was processed within a few hours of death (Fig. 1K), as demonstrated via RT-PCR. Together, these data demonstrate the feasibility of retinal organ culture from human donors.

AAV serotypes display variable transduction of the ONL of human donor retinas

Once the culture methodology was established, the study next asked whether *ex vivo* organotypic explants could be used to test the transduction efficiency of different AAV2 serotypes. To that end, ONL transduction efficiency was assessed in retinal explants from three independent human donor eyes (Table 1, Donor Eyes 2–4) from individuals aged 84 (Fig. 2), 96 (Fig. 3), and 56 years (Fig. 4). Notably, the transduction efficiencies of some serotypes were consistent across the three different donor eyes, whereas others displayed high inter-donor variability. The most consistent transduction efficiencies from capsid serotypes across all eyes tested were AAV serotypes 1, 4, and 8. AAV1 transduction of the ONL was 16.4% in donor eye 1 (Fig. 2A–A′ and H; 16.4 ± 0.95%), but lower in eyes 2 (Fig. 3A–A′ and H; 10.5 ± 0.9%) and 3 (Fig. 4A–A′ and H; 10.8 ± 1.2%). AAV4 transduction was very consistent and overall displayed the highest efficiency across the three eyes tested. Specifically, AAV4 efficiency was 15.9% (Fig. 2C–C′ and H; 15.9 ± 0.8%), 15.3% (Fig. 3C–C′ and H; 15.3 ± 1.0%), and 14.2% (Fig. 4C–C′ and H; 14.2 ± 0.9%). AAV8 was also consistent across all eyes but had the lowest average transduction efficiency of all serotypes tested, yielding averages of 1.5% (Fig. 2F–F′ and H; 1.5 ± 0.2%), 1.8% (Fig. 3F–F′ and H; 1.8 ± 0.2%), and 1.1% (Fig. 4F–F′ and H; 1.1 ± 0.1%). AAV8 also appeared to show some cone selectivity (Figs. 2F and 4F). AAV2 displayed highly variable transduction efficiencies in each eye, yielding 1.1% in eye 1 (Fig. 2B–B′ and H; 1.1 ± 0.4%), 6.4% in eye 2 (Fig. 3B–B′ and H; 6.4 ± 0.9%), and 10.9% in eye 3 (Fig. 4B–B′ and H; 10.9 ± 0.8%), 10-fold higher than the average transduction efficiency observed in eye 1. AAV5 transduced the ONL consistently in eyes 1 (Fig. 2D–D′ and H; 3.9 ± 1.2%) and 2 (Fig. 3D–D′ and H; 3.0 ± 0.5%), but a transduction efficiency more than fourfold higher was observed in eye 3 (Fig. 4D–D′ and H; 16.5 ± 0.9%). In contrast, AAV6-mediated transduction was lower in eye 1 (Fig. 2E–E′ and H; 4.1 ± 0.9%), but consistently fourfold higher in eyes 2 (Fig. 3E–E′ and H; 15.4 ± 1.6%) and 3 (Fig. 4E–E′ and H; 16.5 ± 0.7%). AAV9 transduced 5.8% of the outer nuclear cells in eye 1 (Fig. 2G–G′ and H; 5.8 ± 0.8%) and 10% in eye 2 (Fig. 3G–G′ and H; 10.0 ± 1.0%), but transduction was much lower in eye 3 (Fig. 4G–G′ and H; 1.6 ± 0.2%).

The tropism of AAV2 serotypes was also investigated in RPE-choroid organ cultures from the same donor eye (age 96 years) used for the retinal explants shown in Fig. 3. RPE-choroid cultures incubated with AAV1 showed minor-to-moderate GFP labeling of the RPE and a population of cells in the choroidal stroma (Supplementary Fig. S1A–C). These cells, which were also transduced by AAV2, AAV4, AAV6, and AAV9, exhibited a fibroblastic shape with a small number of short dendritic processes (Supplementary Fig. S1B and C, and G and I). While they were frequently in immediate contact with choroidal

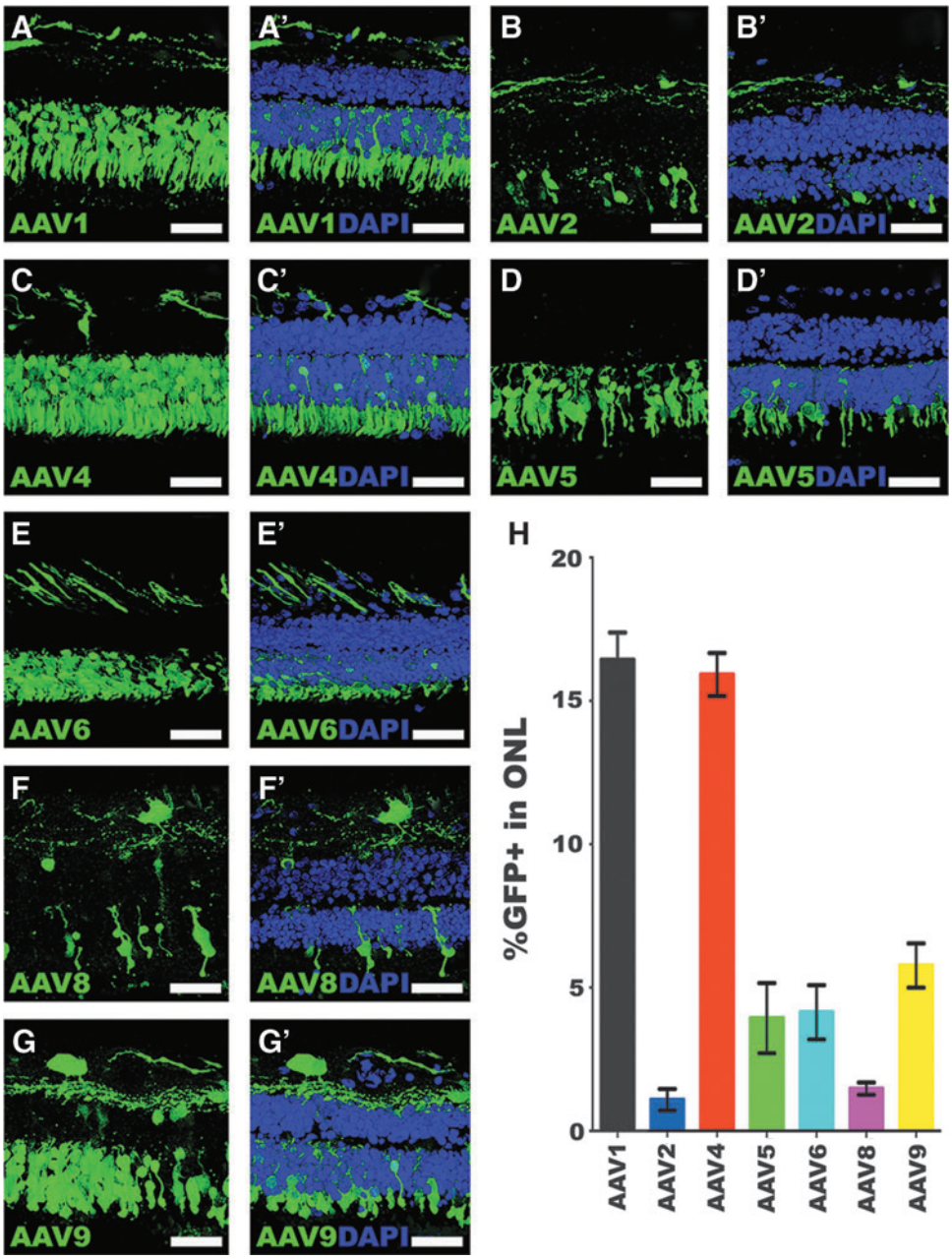

Figure 2. Outer nuclear layer transduction efficiency in retinal explants from an 84-year-old human donor eye. **(A–G′)** Immunohistochemical analysis of green fluorescent protein (GFP) expression (*green*) driven by seven different AAV serotypes. Representative 20 μm z-stacks of retinal explants are shown for each of AAV1 **(A–A′)**, AAV2 **(B–B′)**, AAV4 **(C–C′)**, AAV5 **(D–D′)**, AAV6 **(E–E′)**, AAV8 **(F–F′)**, and AAV9 **(G–G′)**. DAPI was used to visualize retinal nuclei. **(H)** Bar graph displaying the mean % GFP-positive cells in the outer nuclear layer transduced by each AAV serotype. Error bars represent standard error of the mean (SEM). Scale bars = 50 μm.

melanocytes (Supplementary Fig. S1B and C), the GFP-positive cells were not themselves pigmented and did not react with anti-CD45 antibodies. The RPE showed moderate transduction with AAV2 and AAV9 (Supplementary Fig. S1D and I), while more intense anti-GFP labeling was observed for AAV4 and AAV6 (Supplementary Fig. S1E and G). In sections that were dual labeled with the choroidal vascular marker *Ulex europaeus* agglutinin-I, no transduction of choriocapillaris or large vessel choroidal endothelial cells was observed for any of the AAV serotypes tested (data not shown).

Evaluation of inner retinal neurons

When one compares the average ONL transduction efficiency of each AAV serotype across the three donor eyes tested, the high variability of AAVs 2, 5, and 6 is apparent (Fig. 5A). AAV4 and AAV1 dis-

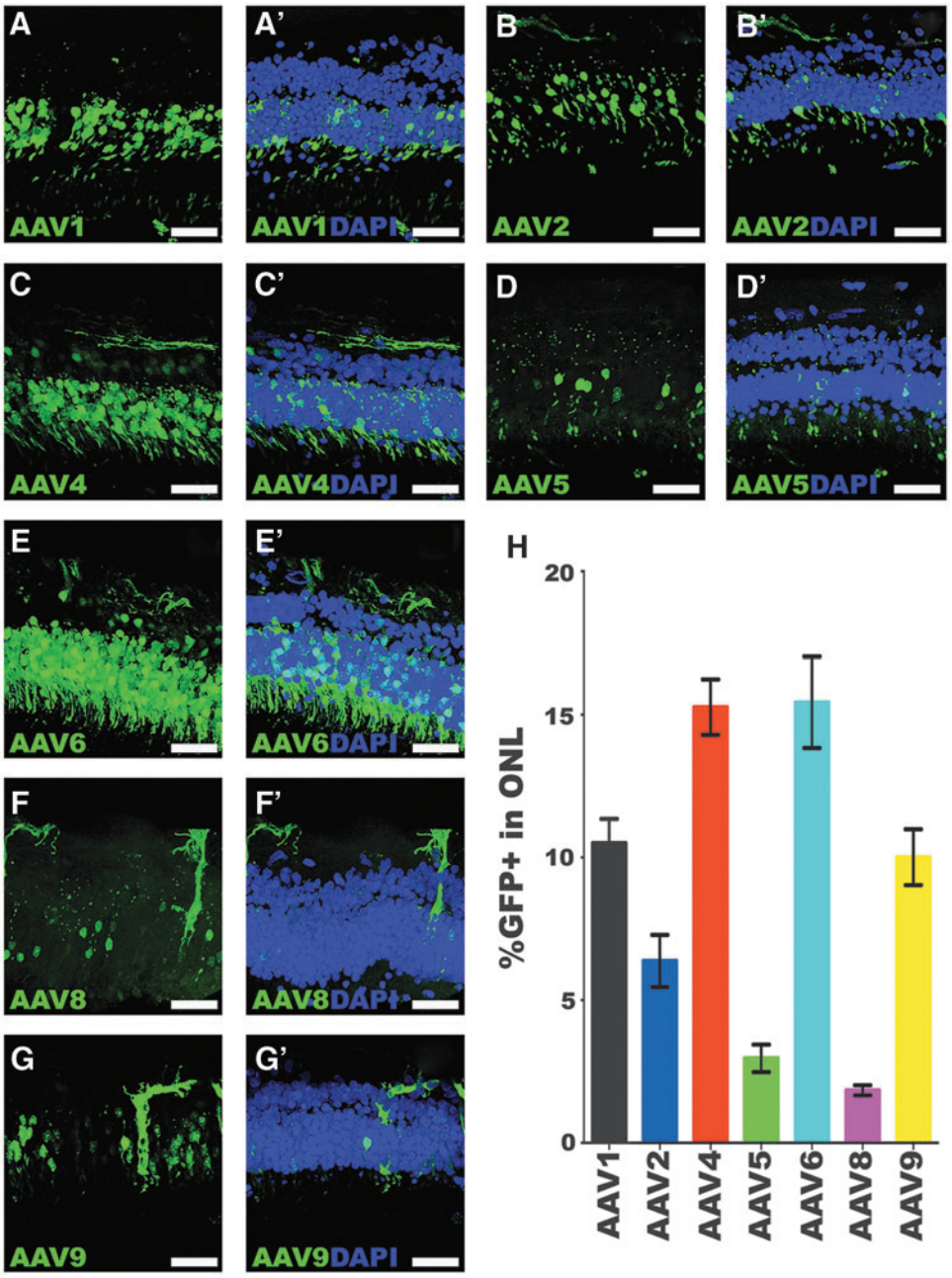

Figure 3. Transduction efficiency of AAV serotypes in retinal explants from a 96-year-old human donor eye. **(A–G′)** Immunohistochemical analysis of GFP expression (*green*) driven by seven different AAV serotypes. Representative 20 μm z-stacks of retinal explants are shown for each of AAV1 **(A–A′)**, AAV2 **(B–B′)**, AAV4 **(C–C′)**, AAV5 **(D–D′)**, AAV6 **(E–E′)**, AAV8 **(F–F′)**, and AAV9 **(G–G′)**. DAPI was used to visualize retinal nuclei. **(H)** Bar graph displaying the mean % GFP-positive cells in the outer nuclear layer transduced by each AAV serotype. Error bars represent SEM. Scale bars = 50 μm.

played the highest overall average transduction efficiencies in the ONL (Fig. 5A). AAVs 5 and 6 were the next highest, but also displayed the largest variability (Fig. 5A). AAVs 2 and 9 produced similar transduction efficiencies, but AAV2 was the more inconsistent of the two serotypes (Fig. 5A). AAV8 was the most consistent and inefficient serotype of the seven tested across all three donor eyes (Fig. 5A). Qualitative observations of tropism in rods versus cones based upon cell morphology of GFP-positive cells did not reveal any obvious preferential transduction of rods or cones by any of the tested serotypes.

In addition to ONL transduction efficiency, the inner retinal tropism of each serotype was also assessed. To do this, the mean percentage of z-stacks analyzed was calculated for each serotype that displayed GFP-positive cells (*i.e.*, AAV-mediated

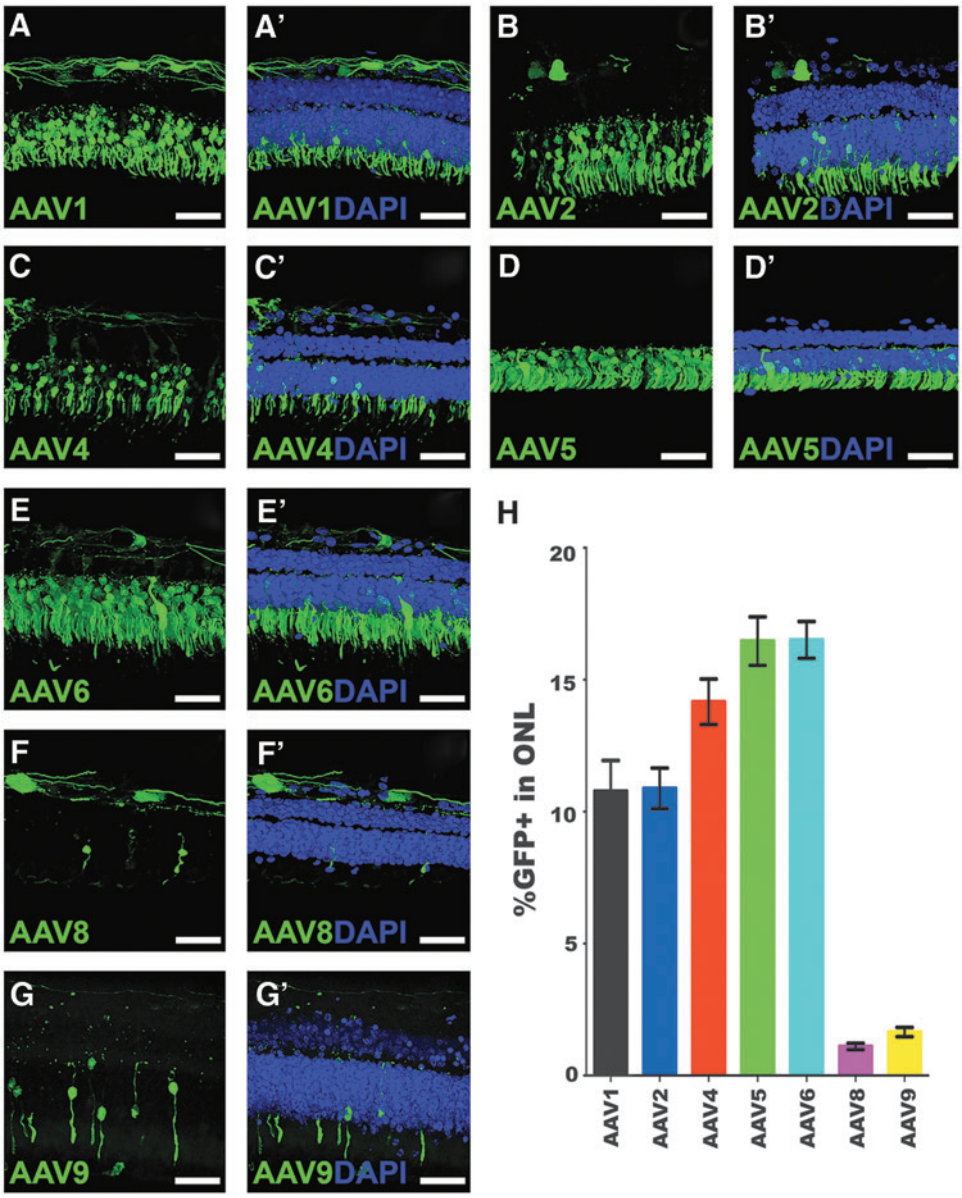

Figure 4. Outer nuclear layer transduction efficiency in retinal explants from a 56-year-old human donor eye. **(A–G′)** Immunohistochemical analysis of GFP expression (*green*) driven by seven different AAV serotypes. Representative 20 μm z-stacks of retinal explants are shown for each of AAV1 **(A–A′)**, AAV2 **(B–B′)**, AAV4 **(C–C′)**, AAV5 **(D–D′)**, AAV6 **(E–E′)**, AAV8 **(F–F′)**, and AAV9 **(G–G′)**. DAPI was used to visualize retinal nuclei. **(H)** Bar graph displaying the mean % GFP-positive cells in the outer nuclear layer transduced by each AAV serotype. Error bars represent SEM. Scale bars = 50 μm.

transduction) within either the INL (Fig. 5B) or the GCL/NFL (Fig. 5C) across the three donor eyes. AAVs 1 and 5 had the lowest INL tropism, whereas AAVs 4 and 6 each displayed GFP expression within the INL in nearly 100% of z-stacks acquired (Fig. 5B). Each AAV serotype transduced cells within the GCL/NFL in most all z-stacks analyzed, with the exception of AAV5 (Fig. 5C). These results suggest that AAV4 and AAV6 displayed the most consistent inner retina tropism overall, while AAV5 transduced the fewest number of inner retinal cells and was largely ONL specific.

Comparison of sub-retinal injection versus treatment of retinal explants in a pig model

To eliminate the possibility that the results observed in human donor retinal explants were due in part to culture artifact (*e.g.*, due to culture condition-induced changes in receptor availability), each serotype was tested in a pig model. To do this, each AAV serotype was injected into three independent eyes of 6-month-old wild-type mini-swine. To reduce the potential for animal-to-animal and eye-to-eye variability, retinal punches were isolated for use as explants from the same

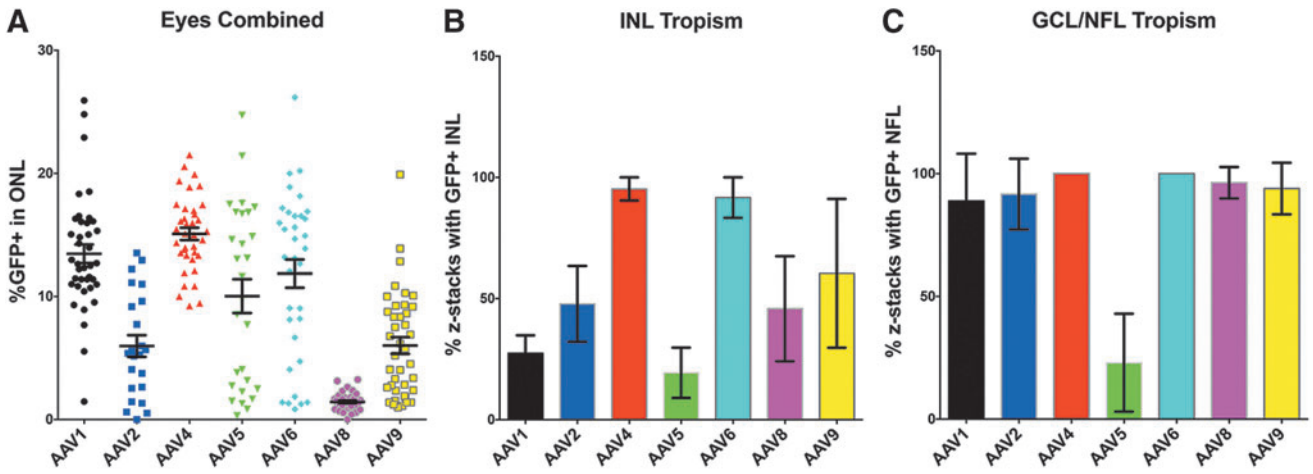

Figure 5. Combined outer nuclear layer transduction efficiency and inner retinal tropism of seven AAV serotypes in retinal explants. **(A)** Dot plot showing all individual data points for the mean % GFP-positive cells in the outer nuclear layer produced by each AAV serotype in all three donor eyes combined. **(B)** Bar graph demonstrating the inner nuclear layer tropism combined for all three donor eyes expressed as the percentage of z-stacks that displayed GFP-positive cells. **(C)** Bar graph demonstrating the ganglion cell layer and nerve fiber layer (GCL/NFL) tropism combined for all three donor eyes expressed as the percentage of z-stacks that displayed GFP-positive cells. Error bars represent SEM (there are no error bars for AAV4 and AAV6 in the GCL/NFL graph because tropism was 100% in all z-stacks assessed across all three eyes).

retinas that received sub-retinal injection (*i.e.*, on the opposite side of the optic nerve from the injection site). Transduction of each AAV serotype was assessed in duplicate organotypic explants from each of three independent eyes. As shown in Fig. 6, representative images for each serotype show that transduction is highly comparable *in vivo* versus *ex vivo*. Notably, transduction by AAV8 was much higher in the pig model than observed in humans, both *in vivo* and *ex vivo*, suggesting that the inefficient transduction efficiency driven by AAV8 in human retinal explants is related to species differences and not due to inadequate quality or quantity of virus.

DISCUSSION

This study describes the development of a human retinal organotypic explant system that allows for the testing of viral vectors in fresh human retina. The assessment of seven different AAV serotypes shows that the transduction efficiency of the ONL (*i.e.*, photoreceptor cells) is variable across the different serotypes tested. Furthermore, there was a noticeable degree of variability among the independent human donor retinas tested. The study also demonstrates that AAV4 and AAV5 are particularly efficient at transducing photoreceptor cells and that AAV5 transduction is, for the most part, specific to the ONL.

Based upon the results of this study, AAV4 had the highest overall transduction efficiency within the ONL across all three donor eyes. AAV4 also demonstrated a high tropism in the inner nuclear and ganglion cell/nerve fiber layers of the inner neural retina. For some diseases, transduction of neurons throughout the neural retina will likely provide the most therapeutic benefit. An example of a disease in which the entire retina is affected is *CLN3*-associated Batten disease.[29] Delivery of full-length CLN3 to the inner retinal neurons, in addition to photoreceptor cells, could prove more effective in halting the natural history of Batten disease than an AAV that targets photoreceptors only. Further, patients with Batten disease also develop severe CNS degeneration that ultimately results in early death. Identification of an AAV serotype that results in efficacious treatment of inner retinal neurons and ganglion cell fibers that connect to the brain could provide a proof-of-principle for the treatment of CNS neurons at risk. Another example of an inherited disease that would benefit more from treatment with an AAV serotype that transduces the inner retina is the juvenile onset macular disease X-linked retinoschisis, which is caused by mutations in the gene *RS1*.[30] Patients with retinoschisis develop cystic spaces in the retina, predominantly at the level of the inner nuclear and outer plexiform layers within the macula.[31,32] The RS1 protein, retinoschisin, is thought to serve as a cell adhesion protein, which helps to maintain retinal structure.[33] Currently, gene augmentation therapy for retinoschisis is being tested in a Phase I–II clinical trial using the AAV8 capsid serotype (NCT02317887).

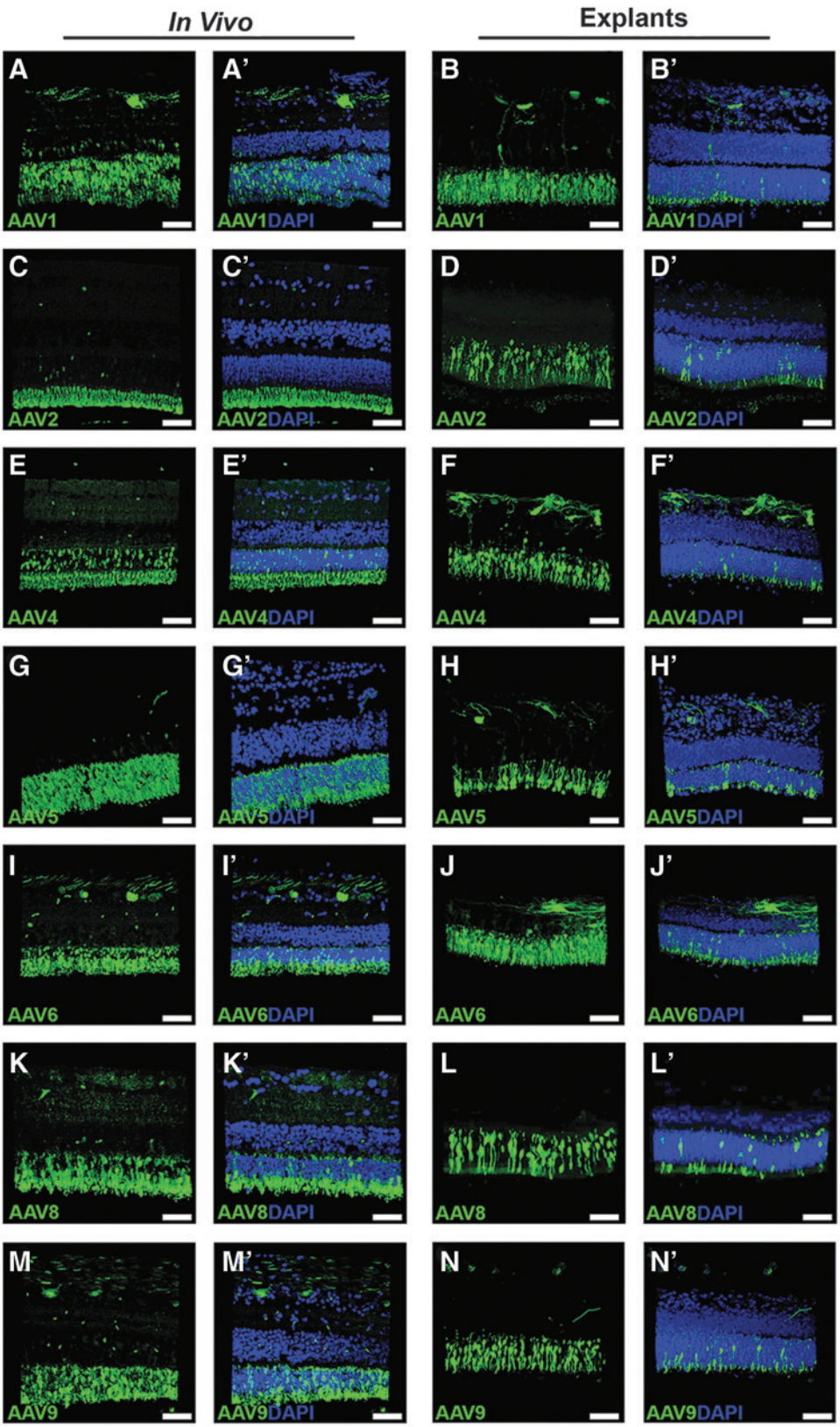

Figure 6. Comparison of AAV serotypes in pig retina: sub-retinal injection versus organotypic explant model. Immunohistochemical analysis of GFP expression (*green*) driven by seven different AAV serotypes. Representative z-stacks of sub-retinally injected (*left side* labeled "*in vivo*") and explanted (*right side* labeled "explants") retinas are shown for each of AAV1 **(A–A′** vs. **B–B′)**, AAV2 **(C–C′** vs. **D–D′)**, AAV4 **(E–E′** vs. **F–F′)**, AAV5 **(G–G′** vs. **H–H′)**, AAV6 **(I–I′** vs. **J–J′)**, AAV8 **(K–K′** vs. **L–L′)**, and AAV9 **(M–M′** vs. **N–N′)**. DAPI was used to visualize retinal nuclei. Scale bars = 50 μm.

For other inherited retinal diseases that specifically affect the photoreceptor cell layer, the data suggest that AAV5 may be the preferred serotype. Although AAV5 displayed noticeable variability in transduction of the ONL across the three human donor eyes tested, this serotype was largely restricted to the photoreceptor cells. For diseases such as *MAK*- and *TRNT1*-associated retinitis pigmentosa,[34–36] both of which are caused by mutations in genes that are small enough to be packaged into AAVs, gene replacement within photoreceptor cells missing functional gene products has the potential to delay or prevent cell death. An additional option may be to engineer an AAV with high transduction efficiency throughout the retina, such as AAV4, with a photoreceptor-specific promoter such as rhodopsin,[37] rhodopsin kinase,[38] or interphotoreceptor-binding protein,[39] instead of the stronger, constitutively active CMV promoter.[40]

Interestingly, in this study, AAV8 consistently produced the lowest transduction efficiency in human photoreceptor cells. While good transduction was observed in the inner retina, few human photoreceptor cells showed viral transduction. This is a notable finding, as others have shown that AAV8 robustly transduces the mouse retina[41,42] and pig retina[9,17] (also observed in the current study, Fig. 6) following sub-retinal injection. This finding highlights the fact that there are important molecular and structural differences between the photoreceptor cells of commonly used animal models and human eyes, and that data from animal models may not always be generalizable for potential human therapies.[43,44] Future studies aimed at investigating the extent to which humans and model organisms differentially express receptors for AAV8 and other AAVs are warranted.[45,46]

Another noteworthy observation from this study is that considerable variability was seen in the transduction efficiency of the ONL for each serotype (excluding AAV8) across the three different human donor eyes tested. This study tested eyes from individuals representing three different decades of life, aged 56, 84, and 96 years, suggesting that there may be donor-to-donor or age-dependent differences in reception to transduction. Maguire *et al*. found age-dependent effects in patients administered AAV2-*RPE65*, with the greatest improvements in vision observed in children.[3] While it is likely that this finding is at least partially the result of the fact that children being treated earlier in the course of disease have not experienced as much photoreceptor cell death, a difference in age-dependent uptake of AAV2 is also a possibility. Although difficult to perform given the limited availability of fresh human donor eyes, assessing transduction and tropism from multiple eyes across multiple decades would be highly valuable to the clinical and scientific communities. Identifying vector serotypes that remain consistent regardless of age would allow for treatment of thousands of individuals. In 2012, Baba *et al*. investigated the cell-specific tropism of AAVs 1, 8, and 9 in mouse and marmoset retinal explants at different stages of development.[47] They observed that tropism in younger retinal explants was similar in each species, with transduction primarily in inner retinal cells such as amacrine and horizontal cells but very few photoreceptors, whereas photoreceptor tropism was increased in adult retinal explants. In contrast, a decrease in inner retinal transduction has been described for systemically delivered AAV9 in mice.[48] A more comprehensive understanding of how age affects viral uptake by human retinal cells would therefore be valuable to the field.

In addition to retinal explants, this study also demonstrates the tropism of AAV serotypes in RPE-choroid organ cultures. Administration of AAV serotypes to RPE-choroid organ cultures showed that the RPE was transduced the strongest by AAV4 and AAV6. While transduction of the endothelial cells of either the choriocapillaris or larger choroidal vessels was not observed by any of the seven serotypes, AAVs 2, 4, 6, and 9 did result in GFP expression in a population of cells in the choroidal stroma. Although the exact identity of these cells has not yet been determined, they are non-pigmented, in close contact with choroidal melanocytes, and do not positively label with immune cell-specific antibody (anti-CD45). In light of a growing body of evidence for immune-mediated choroidal injury early in diseases such as age-related macular degeneration (AMD),[49] tools to target the choroid will be essential for future interventions. Although further investigation is warranted, the results shown here raise the possibility of using AAVs to deliver factors that could potentially protect the choriocapillaris from harm, for example in patients with the high-risk complement factor H genotype associated with AMD.

This study has some limitations. Unlike inbred strains utilized in studies of animal model systems, humans are heterogenous, both genetically and with respect to environmental exposures, and thus greater individual-to-individual variability is expected. Indeed, while the overall patterns were shared, variability of transduction efficiency was observed between the human donor eyes tested. Future experiments may expand this study by assessing equal numbers of male and female donor

eyes at multiple decades of life and with different disease states.

In conclusion, this study demonstrates the use of human retinal explants for testing the transduction efficiency and tropism of different AAV serotypes. This approach may allow the identification of the optimal AAV serotypes to use for different inherited retinal diseases. This study also demonstrates that there is variability among individual eyes treated *in vitro*. Comparison of results in human retinas to those observed in mice suggest that while animal models are useful for initial studies assessing the usefulness of AAVs, their results can be misleading with respect to how they may or may not fare when administered to human retina.

ACKNOWLEDGMENTS

The authors would like to thank the eye donors and their families for their extremely valuable role in biomedical research. The authors gratefully acknowledge the Iowa Lions Eye Bank for their continued support of vision research. Grant support: The Stephen A. Wynn Foundation, The Elmer and Sylvia Sramek Charitable Foundation, and National Institutes of Health Grants (NIH; Bethesda, MD): EY024605, EY024588, EY026008, and P30 EY025580.

AUTHOR DISCLOSURE

No competing financial interests exist for any of the authors included in this manuscript.

REFERENCES

1. Stone EM, Andorf JL, Whitmore SS, et al. Clinically focused molecular investigation of 1000 consecutive families with inherited retinal disease. Ophthalmology 2017;124:1314–1331.
2. Acland GM, Aguirre GD, Ray J, et al. Gene therapy restores vision in a canine model of childhood blindness. Nat Genet 2001;28:92–95.
3. Maguire AM, High KA, Auricchio A, et al. Age-dependent effects of *RPE65* gene therapy for Leber's congenital amaurosis: a Phase 1 dose-escalation trial. Lancet 2009;374:1597–1605.
4. Stein L, Roy K, Lei L, et al. Clinical gene therapy for the treatment of *RPE65*-associated Leber congenital amaurosis. Expert Opin Biol Ther 2011; 11:429–439.
5. Jacobson SG, Cideciyan AV, Ratnakaram R, et al. Gene therapy for Leber congenital amaurosis caused by *RPE65* mutations: safety and efficacy in 15 children and adults followed up to 3 years. Arch Ophthalmol 2012;130:9–24.
6. Maguire AM, Simonelli F, Pierce EA, et al. Safety and efficacy of gene transfer for Leber's congenital amaurosis. N Engl J Med 2008;358:2240–2248.
7. Auricchio A, Kobinger G, Anand V, et al. Exchange of surface proteins impacts on viral vector cellular specificity and transduction characteristics: the retina as a model. Hum Mol Genet 2001;10:3075–3081.
8. Stieger K, Lhériteau E, Moullier P, et al. AAV-mediated gene therapy for retinal disorders in large animal models. ILAR J 2009;50:206–224.
9. Mussolino C, della Corte M, Rossi S, et al. AAV-mediated photoreceptor transduction of the pig cone-enriched retina. Gene Ther 2011;18:637–645.
10. Zincarelli C, Soltys S, Rengo G, et al. Analysis of AAV serotypes 1–9 mediated gene expression and tropism in mice after systemic injection. Mol Ther 2008;16:1073–1080.
11. Natkunarajah M, Trittibach P, McIntosh J, et al. Assessment of ocular transduction using single-stranded and self-complementary recombinant adeno-associated virus serotype 2/8. Gene Ther 2008;15:463–467.
12. Surace EM, Auricchio A, Reich SJ, et al. Delivery of adeno-associated virus vectors to the fetal retina: impact of viral capsid proteins on retinal neuronal progenitor transduction. J Virol 2003;77: 7957–7963.
13. Petrs-Silva H, Dinculescu A, Li Q, et al. High-efficiency transduction of the mouse retina by tyrosine-mutant AAV serotype vectors. Mol Ther 2009;17:463–471.
14. Watanabe S, Sanuki R, Ueno S, et al. Tropisms of AAV for subretinal delivery to the neonatal mouse retina and its application for *in vivo* rescue of developmental photoreceptor disorders. PLoS One 2013;8:e54146.
15. Bogner B, Boye SL, Min S-H, et al. Capsid mutated adeno-associated virus delivered to the anterior chamber results in efficient transduction of trabecular meshwork in mouse and rat. PLoS One2015;10:e0128759.
16. Colella P, Trapani I, Cesi G, et al. Efficient gene delivery to the cone-enriched pig retina by dual AAV vectors. Gene Ther 2014;21:450–456.
17. Manfredi A, Marrocco E, Auppo A, et al. Combined rod and cone transduction by adeno-associated virus 2/8. Hum Gene Ther 2013;24: 982–992.
18. Stieger K, Schroeder J, Provost N, et al. Detection of intact rAAV particles up to 6 years after successful gene transfer in the retina of dogs and primates. Mol Ther 2009;17:516–523.
19. Bruewer AR, Mowat FM, Bart JT, et al. Evaluation of lateral spread of transgene expression following subretinal AAV-mediated gene delivery in dogs. PLoS One 2013;8:e60218.
20. Mowat FM, Gornik KR, Dinculescu A, et al. Tyrosine capsid-mutant AAV vectors for gene delivery to the canine retina from a subretinal or intravitreal approach. Gene Ther 2014; 21:96–105.
21. Charbel Issa P, De Silva SR, Lipinski DM, et al. Assessment of tropism and effectiveness of new primate-derived hybrid recombinant AAV serotypes in the mouse and primate retina. PLoS One 2013;8:e60361.
22. Koilkonda RD, Hauswirth WW, Guy J. Efficient expression of self-complementary AAV in ganglion cells of the *ex vivo* primate retina. Mol Vis 2009; 15:2796–2802.
23. Boye SE, Alexander JJ, Witherspoon CD, et al. Highly efficient delivery of adeno-associated viral vectors to the primate retina. Hum Gene Ther 2016;27:580–597.
24. Boye SE, Alexander JJ, Boye SL, et al. The human rhodopsin kinase promoter in an AAV5 vector confers rod- and cone-specific expression in the primate retina. Hum Gene Ther 2012;23:1101–1115.
25. Vandenberghe LH, Auricchio A. Novel adeno-associated viral vectors for retinal gene therapy. Gene Ther 2012;19:162–168.
26. Chirco KR, Whitmore SS, K Wang K, et al. Monomeric C-reactive protein and inflammation in age-related macular degeneration. J Pathol 2016; 240:173–183.
27. Wiley LA, Beebe DC, Mullins RF, et al. A method for sectioning and immunohistochemical analysis of stem cell–derived 3-D organoids. Curr Protoc Stem Cell Biol 2016;37:1C.19.1–1C.19.11.
28. Mullins RF, Johnson MN, Faidley EA, et al. Choriocapillaris vascular dropout related to den-

sity of drusen in human eyes with early age-related macular degeneration. Invest Ophthalmol Vis Sci 2011;52:1606–1612.

29. Bensaoula T, Shibuya H, Katz ML, et al. Histopathologic and immunocytochemical analysis of the retina and ocular tissues in Batten disease. Ophthalmology 2000;107:1746–1753.
30. Sauer CG, Gehrig A, Warneke-Wittstock R, et al. Positional cloning of the gene associated with X-linked juvenile retinoschisis. Nat Genet 1997;17: 164–170.
31. Sieving PA, Yashar BM and R Ayyagari. Juvenile retinoschisis: a model for molecular diagnostic testing of X-linked ophthalmic disease. Trans Am Ophthalmol Soc 1999;97:451–464; discussion 464–469.
32. Gao H, Kusumi R, Yung C-W. Optical coherence tomographic findings in X-linked juvenile retinoschisis. Arch Ophthalmol 2005;123:1006–1008.
33. Weber BHF, Schrewe H, Molday LL, et al. Inactivation of the murine X-linked juvenile retinoschisis gene, *Rs1h*, suggests a role of retinoschisin in retinal cell layer organization and synaptic structure. Proc Natl Acad Sci U S A 2002; 99:6222–6227.
34. Tucker BA, Scheetz TE, Mullins RF, et al. Exome sequencing and analysis of induced pluripotent stem cells identify the cilia-related gene male germ cell-associated kinase (MAK) as a cause of retinitis pigmentosa. Proc Natl Acad Sci U S A 2011;108:E569–576.
35. Whitmore SS, Wagner AH, DeLuca AP, et al. Transcriptomic analysis across nasal, temporal, and macular regions of human neural retina and RPE/choroid by RNA-Seq. Exp Eye Res 2014;129: 93–106.
36. DeLuca AP, Whitmore SS, Barnes J, et al. Hypomorphic mutations in *TRNT1* cause retinitis pigmentosa with erythrocytic microcytosis. Hum Mol Genet 2016;25:44–56.
37. Dalkara D, Byrne LC, Lee T, et al. Enhanced gene delivery to the neonatal retina through systemic administration of tyrosine-mutated AAV9. Gene Ther 2012;19:176–181.
38. Sun X, Pawlyk B, Xu X, et al. Gene therapy with a promoter targeting both rods and cones rescues retinal degeneration caused by *AIPL1* mutations. Gene Ther 2010;17:117–131.
39. Boyd RF, Sledge DG, Boye SL, et al. Photoreceptor-targeted gene delivery using intravitreally administered AAV vectors in dogs. Gene Ther 2016;23: 400.
40. Thomsen DR, Stenberg RM, Goins WF, et al. Promoter-regulatory region of the major immediate early gene of human cytomegalovirus. Proc Natl Acad Sci U S A 1984;81:659–663.
41. Igarashi T, Miyake K, Asakawa N, et al. Direct comparison of administration routes for AAV8-mediated ocular gene therapy. Curr Eye Res 2013; 38:569–577.
42. Black A, Vasireddy V, Chung DC, et al. Adeno-associated virus 8-mediated gene therapy for choroideremia: preclinical studies in *in vitro* and *in vivo* models. J Gene Med 2014;16:122–130.
43. Perel P, Roberts I, Sena E, et al. Comparison of treatment effects between animal experiments and clinical trials: systematic review. *BMJ* 2007; 334:197.
44. Kostic C, Arsenijevic Y. Animal modelling for inherited central vision loss. J Pathol 2016;238: 300–310.
45. Akache B, Grimm D, Pandey K, et al. The 37/67-kilodalton laminin receptor is a receptor for adeno-associated virus serotypes 8, 2, 3, and 9. J Virol 2006;80:9831–9836.
46. Nonnenmacher M, Weber T. Intracellular transport of recombinant adeno-associated virus vectors. Gene Ther 2012;19:649–658.
47. Baba Y, Satoh S, Otsu M, et al. *In vitro* cell subtype-specific transduction of adeno-associated virus in mouse and marmoset retinal explant culture. Biochimie 2012;94:2716–2722.
48. Bostick B, Ghosh A, Yue Y, et al. Systemic AAV-9 transduction in mice is influenced by animal age but not by the route of administration. Gene Ther 2007;14:1605–1609.
49. Mullins RF, Schoo DP, Sohn EH, et al. The membrane attack complex in aging human choriocapillaris: relationship to macular degeneration and choroidal thinning. Am J Pathol 2014;184: 3142–3153.

Received for publication September 4, 2017; accepted after revision November 19, 2017.

Published online: November 20, 2017.